Modelling of flexural response of simply supported RC skew slab

Madhu Sharma[1,*], Naveen Kwatra[1] and Harvinder Singh[2]

[1]Department of Civil Engineering, Thapar Institute of Engineering and Technology, Patiala 147 001, India
[2]Department of Civil Engineering, Guru Nanak Dev Engineering College, Ludhiana 141 006, India

Skew slabs have various applications, e.g. as floor of bridges and buildings. This is pertinent when it is not possible to cross a river or gap at an angle of 90°. Design aids and plans suggested by various codes are applicable for standard skew angles, i.e. 15°, 30°, 45°, etc. with selective spans only. However, in actual practices, several cases are encountered, wherein skew angle and aspect ratio of the slab panel do not fit the recommended guidelines. This occurs due to the very high land cost and space limitations. The present study proposes an analytical model for the design of skew slabs with any skew angle and aspect ratio. The developed model indicates that skew slabs simply supported along two opposite parallel sides and free along the other two sides are suitable for the construction of bridges having short diagonal larger than the span. The developed model validates the assumptions considered in terms of collapse loads and crack patterns experimentally and numerically. This shall facilitate engineers during the design of skew slab bridge for any skew angle and aspect ratio, without deviating from the alignment of the road.

Keywords: Finite-element analysis, flexural response, skew slabs, yield-line method.

SKEW slabs have various applications in structures, particularly in bridges. These slabs are planned to cover the gap where the crossing is not at an angle of 90°. This occurs due to many reasons, such as non-availability of land or congested urban areas. The design of any reinforced concrete (RC) slab is governed by moment field induced in the slab due to the applied load. This moment field in the skew slabs changes significantly due to various influencing factors, i.e. skew angle, slab aspect ratio and boundary conditions. The inclination of the centre line of the slab to the horizontal axis is measured as the skew angle, whereas the ratio of supported length to unsupported length of the slab is known as the aspect ratio.

It is an established fact that a skew slab exhibits an entirely different response upon loading in comparison to the rectangular slab even with identical boundary conditions. A large number of factors have been found to control the behaviour of skew slabs, such as skew angle, slab aspect ratio, support conditions, etc. Hence the skew slab behaves like a highly redundant structural system which displays some special characteristics. First, significant torsional moments are induced in the slab. Secondly, the longitudinal moment starts decreasing with an increase in the transverse moment. The corners of the slab exhibit uplifting depending upon the skewness. The above-mentioned characteristics add more complexities while designing a skew slab over a rectangular slab. According to the American and Indian codes, i.e. the American Association of State Highway and Transportation Officials (AASHTO)[1] and Ministry of Road and Transport (road wing). Indian Road Congress (IRC), the guidelines available for analysis and design of skew slabs are applicable for some recommended range or limit only. AASTHO (ref. 1) recommends a correction factor for the evaluation of distribution factor for the live load bending moment, which reduces the bending moment for larger skew angles and overestimates the maximum moment by 20–100% for skew angles of 30°–50° (ref. 2). Whereas the bending moment coefficients and plans suggested by IRC[3] become irrelevant for analysis and design of bridges with skew angle as high as 85° and as low as 10°. These guidelines are applicable only for standard skew angles, i.e. 15°, 30°, 45° and 60° with selective spans based on the number of lanes[3]. The designer has no other alternative than choosing one of the suggested skew slab bridges which is closer to the actual angle of skew desired at the site.

Studies are in progress on to establish a link between various influencing factors, i.e. skew angle, aspect ratio and boundary conditions to formulate simple design procedures and charts for analysis of skew slabs. In previous studies, various methods were used to design skew slabs such as 'equivalent beam method' or 'grillage model[4–6], where the slab was represented by two strips across the slab width and length. Equivalent beam method has been used since 1930 for the design of skew slabs. The provisions and guidelines suggested by AASHTO codes are also based on this method, but it always gives moment field on conservative side[6]. The grillage method gives a more refined model compared to the equivalent beam method, but it is limited to two-dimensional analysis and the moment field depends on fineness and orthogonality of the mesh. Although these

*For correspondence. (e-mail: gautamadhu@gmail.com)

methods provide a satisfactory solution to the problem, they come with inherent errors in the form of assumptions. Moreover, these cannot be applied blindly; the designer has to follow the boundaries defined by the assumptions of the study. Researchers have[2,7] recommended three-dimensional finite element (FE) method to analyse skew slabs for more accurate results; however, the FE method is time-consuming. Therefore, there is a need to develop a simple procedure or methodology so to design skew slabs with any desired degree of skew angle.

The design of any RC slab is based on ultimate limit state principles. Design aides of British and Indian codes have used Johansen's yield line analysis for the determination of moment coefficient to evaluate the design values for rectangular/square slabs. Several researchers[8–10] have utilized yield criterion for rectangular slabs to predict the collapse load. However, little attention has been paid to employ this method on skew slabs, as the European Concrete Building Project at Cardington, UK, which tested a variety of methods of designing slabs, found that yield line design generates economic concrete slabs with low amounts of reinforcement. In this study, an analytical model for skew slab resting over simple supports with any skew angle and aspect ratio has been developed. The same has been validated experimentally and numerically utilizing nonlinear analysis software tool.

Research significance

In recent times, the major thrust in the transport sector is construction of more roads, bridges and culverts, etc. Accordingly, the Government of India (GoI) has taken a major initiative in highway development through NHDP, State highway improvement programmes, Pradhan Mantri Gram Sadak Yojana and port connectivity. Also, vehicular traffic in both urban and rural areas has been increased manifold in recent years due to awareness towards mobility through their vehicles to save time.

As a structural designer or highway planner, the most common issue or complexity while designing a river-crossing, highway interchange or grade separator is space limitation or site alignment. The escalating land costs near a bridge site or proximity of the site area to places of religions worship and restrictions on their demolition, compels a designer to propose a skew slab instead of a rectangular slab. The available approaches/methodologies to design a skew slab come with an inherent limitation, viz. the geometry of the road projects at the skew crossing is disturbed if the actual angle of the skew bridge at the site is different from those recommended by IRC 1983. So, there is a need for a general-purpose analytical tool that can tackle these kinds of practical constraints and can provide a free hand to engineers to design skew slab bridges for any angle and aspect ratio without deviating from the alignment of the road. The proposed analytical model and design methodology can be a supplement to the design aids published by IRC 1983 through the Ministry of Shipping and Transport, GoI, and give a rational and economic skew slab system.

Collapse mechanism

To predict the mode of collapse mechanism, thermocol sheets were used in the skew slab model with different skew angles and aspect ratios. The different profiles of thermocol skew slab models were studied under the action of concentrated load at the centre. It was observed that when the ratio of short diagonal to span of the skew slab was kept less than unity ($L/l < 1$), there was some uplifting at the acute (angle <90°) corners; otherwise there was no uplifting. This is because, in the case of simple supports, the reactions $R1$ and $R2$ act on a line through the centre, which forms an angle θ with b. When $L > l$, the reactions are located inside the supports (Figure 1 *b*). When $L < l$, they are outside, but the slab rotates about the axis b' at an angle θ with short diagonal and the reactions act only at the obtuse corners (Figure 1 *a*). As the point load at the centre is increased, the skew slab behaves elastically up to the stage at which tensile reinforcement in the central part of the slab, the area of maximum moment, begins to yield. This causes small cracks on the tensile face of the slab at the centre. If the slab is under-reinforced with respect to failure, then the cracked section will continue to deform without any appreciable increase in moment. As a result, increase in slab load will cause the steel in adjacent sections to yield as well, and the yield lines will extend progressively parallel to the support b or axis of rotation b', as the case may be, until they reach the boundary of the slab. At this stage, since the yield lines can propagate no further, and the resistance moments along the yield lines are almost at their ultimate values; the slab now carries the maximum load possible. Any further increase in load will cause excessive deflection and crushing of the concrete at some sections of the yield lines, leading to over-loading of the rest of the slab and complete collapse. Therefore when a point load is applied at the centre of the simply supported under-reinforced skew slab of short diagonal (L) less than the span (l) and increased further. Then the positive yield line should develop on tensile face of slab starting at the centre and extending up to the free edges of the slab parallel to the lines of rotation EC and BF in Figure 2 *a* at an angle equal to the acute angle of the slab as shown. The slab is divided into two segments between the axis of rotation. Slab segments beyond the axis of rotation towards supports lift up the acute corners A and D. In the case when a point load is applied at the centre of the simply supported skew slab of short diagonal (L) greater than the span (l) and gradually increased. The positive yield line should develop on the tensile face of the slab at

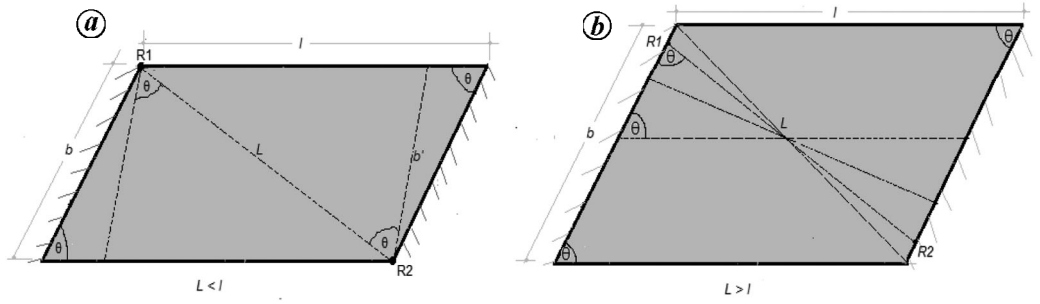

Figure 1. Reactions of skew slab simply supported on two opposite sides (***a***) $L < l$ and (***b***) $L > l$.

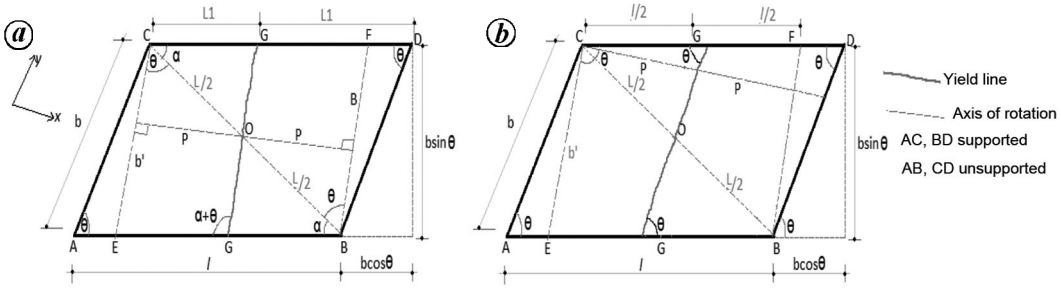

Figure 2. Yield-line pattern of skew slabs. (***a***) Short diagonal to span less than unity. (***b***) Short diagonal to span greater than unity.

collapse, parallel to the supports starting through the centre and extending up to the free edges of the slabs (Figure 2 *b*) dividing the slab into two segments that rotate about the supports.

Design equation

Since the length of short diagonal depends on the skew angle of the slab and its length of support, therefore three of the values, i.e. skew angle, length of support and span along the traffic together decide the type of skew slab and its yield pattern under collapse load. Consider a skew slab having a length (l) and width (b) in the analysis for both cases ($L < l$ and $L > l$) with aspect ratio r ($=b/l$). The skewness of the slab is represented by an acute angle of the skew slab (θ) = (90° – skew angle) measured from the horizontal axis and the slab rests over the simple supports on its two opposite edges (AC and BD; Figure 2). It is reinforced with main reinforcement at the bottom face of the slab at right angles to the supports, i.e. the along x-direction and distribution reinforcement laid over main reinforcement, parallel to the supports, i.e. along the y-direction.

Skew slab, $L < l$

When a uniformly distributed load is applied to an under reinforced concrete, simply supported skew slab of short diagonal (L) less than the span (l) up to the ultimate stage, the positive yield line developed on the tensile face of the slab as shown in Figure 2 *a*. The formation of this yield line started from the centre and extending towards the free edges, parallel to the lines of rotation *CE* and *BF* at an angle, equal to the acute angle, from the short diagonal of the slab. The slab was divided into two segments between the axis of rotation. Slab segments beyond the axis of rotation towards the supports lift up at the acute corners *A* and *D*. The work done by the external load can be determined by multiplying the load (w) by a corresponding distance (δ) moved in the direction of the load given in eq. (1) below.

External work done, $We = \Sigma w\delta$.

$(L) = (l^2 + b^2 - 2lb\cos\theta)^{0.5}$,

$b' = Lr$ = length of yield line.

$$We = wb'L\sin\theta\frac{\delta}{2}. \quad (1)$$

The total internal work done (IWD) by the positive moment field, representing contribution from both the segments of the collapse mechanisms, can be obtained by summing up their individual contributions, given below in eq. (2) below.

$$Wi = 2Mb'\theta',\ Wi = 2Mb'\frac{2\delta}{(L\sin\theta)}. \quad (2)$$

Now equating the external work done to the internal energy absorbed, i.e. eq. (1) = eq. (2).

$$M = \frac{[wl^2 \sin^2\theta(1-2r\cos\theta+r^2)]}{8}. \quad (3)$$

Since yield line makes an angle $(180-(2\theta+\alpha))$ with the line at right angles to the reinforcement, therefore, ultimate moment per unit of length is given in eq. (4) below.

$$M = M_X l^2 \frac{\left\{\begin{array}{c}4r\sin^2\theta\cos\theta+4r^2\sin^2\theta\cos^4\theta \\ +(1-r\cos\theta)^2(1-\sin^2 2\theta)\end{array}\right\}}{(l^2+b^2-2lb\cos\theta)}.$$

$$M = M_X\alpha_1.$$

$$\alpha_1 = \frac{l^2\left\{\begin{array}{c}4r\sin^2\theta\cos\theta+4r^2\sin^2\theta\cos^4\theta \\ +(1-r\cos\theta)^2(1-\sin^2 2\theta)\end{array}\right\}}{(l^2+b^2-2lb\cos\theta)}.$$

Substituting the value of α_1 in eq. (3),

$$M_X = \frac{[wl^2\sin^2\theta(1-2r\cos\theta+r^2]}{8\alpha_1}. \quad (4)$$

For point load applied at the centre

$$We = W\delta. \quad (5)$$

$$Wi = 2b'M\left(\frac{2\delta}{L\sin\theta}\right). \quad (6)$$

Now equating the external work done to the internal energy absorbed, i.e. eq. (5) = eq. (6).

$$\frac{W}{M_X} = \frac{4r\alpha_1}{\sin\theta}. \quad (7)$$

Skew slab, L>l

When a uniformly distributed loaded is applied on the simply supported skew slab of short diagonal (L) greater than the span (l) and gradually increased, then a positive yield line should develop on the tensile face of the slab at collapse, parallel to the supports starting through the centre and extending up to the free edges of the slab as shown in Figure 2 *b*, dividing the slab into two segments that rotate about the supports. Since yield line is at right angles to the reinforcement $M = M_X$.

$$We = \sum w\delta,\ 2w\left(\frac{l}{2}\right)b\sin\theta\left(\frac{\delta}{2}\right). \quad (8)$$

$$Wi = \frac{2Mb2\delta}{(l\sin\theta)} = 4M_X\frac{b\delta}{(l\sin\theta)}. \quad (9)$$

After equating the $We = Wi$,

$$M_X = \frac{(wl^2\sin^2\theta)}{8}. \quad (10)$$

For point load

$$\frac{W}{M_X} = \frac{4r}{\sin\theta}. \quad (11)$$

Equations (7) and (11) are solved to determine the slab moment for $L < l$ and $L > l$ respectively.

Experimental validation

In order to confirm the validity of assumptions and other parameters (aspect ratio and skew angle) of the analytical work, an extensive experimental study was conducted. An experimental set-up was made to maintain the compatibility of test slab specimens with the available reaction frame of 1000 kN. The main parameters studied were collapse load, failure pattern/yield line and load/deflection response.

Details of materials

Ordinary Portland cement conforming to IS 8112 (ref. 11) with fine aggregate (river sand with specific gravity 2.62) conforming to zone III of IS 383 (ref. 14) and crushed coarse aggregates was used to prepare concrete for the casting of slab specimens. The maximum size of course aggregate (specific gravity 2.82) was limited to 12.5 due to smaller slab section. Cement–concrete mix of grade M25 and steel bar with a yield strength of 415 MPa were used to cast the test specimens. The concrete mix proportion was found to be 1 : 1.58 : 2.56 with w/c ratio 0.5 according to the Indian standard (ref. 15). The characteristic compressive strength of size 150 mm cube after 28 days is obtained as 32.2 MPa.

Casting of skew slab specimens

In order to justify the analytical results of the proposed design equations for both cases, the skew slab simply supported on two opposite sides can be divided into two types depending on the shape and behaviour: (i) skew slab with ratio of short diagonal to span less than unity ($L < l$) and (ii) skew slab with ratio of short diagonal to span greater than unity ($L > l$), where L is the short diagonal and l is the span. Two test slabs were casted

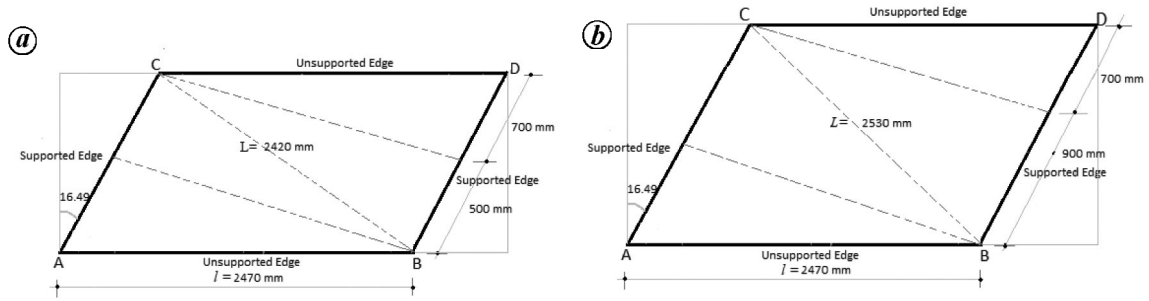

Figure 3. Skew slab specimens with dimension: (***a***) short diagonal less than span ($L < l$) and (***b***) short diagonal greater than span ($L > l$).

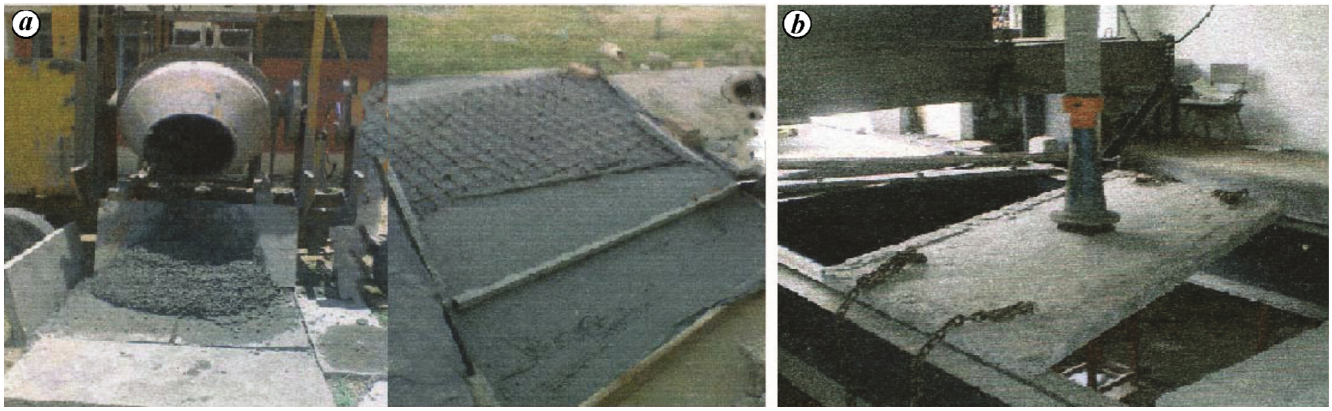

Figure 4. Operation of casting and testing of skew slab specimens: (***a***) casting and (***b***) testing.

Table 1. Summary of test slabs

Skew slab type	Skew slab size (mm)	Short diagonal length (mm)	Skew angle θ (°)	Reinforcement details		Material properties
				Right angle to supports of slab (mm)	Parallel to the supports of slab (mm)	
$L < l$	2470 × 1200 × 70	2420	16.49°	8 Ø 100	8 Ø 125	M-25 grade concrete, Fy-415 steel
$L > l$	2470 × 1600 × 70	2530	16.49°	8 Ø 100	8 Ø 125	

with skew angle of 16.49° and aspect ratio of 0.49 and 0.65 to keep short diagonal less than and greater than the span respectively (Figure 3 *a* and *b*). M25 grade of concrete and Fe 415 steel were used for casting of test slabs. The slabs were reinforced with main reinforcement of 8 mm diameter @ 100 mm at the bottom face of the slab at right angles to the supports, i.e. along the *x*-direction and distribution reinforcement of 8 mm diameter tor steel bars @ 125 mm laid over the main reinforcement parallel to the supports, i.e. along the *y*-direction. Table 1 provides a summary of both the test slabs. The casting of both skew slabs was done on a specifically prepared (level) bed (Figure 4 *a*). Dimensions of the skew slabs were marked on the levelled bed and rebars were placed on the ground with a clear cover of 10 mm. Next, concrete was poured in the prepared mould and levelled to attain a uniform thickness of 70 mm by a trowel and levelling bar. A rod vibrator was used for proper compaction of the concrete to obtain the required size of slabs. After casting, the process of water curing was started for 28 days.

Testing of skew slab specimens

After 28 days of curing, the skew slab specimens were tested on the reaction frame. Slab specimens were lifted with the arrangement of crane and transferred to the reaction frame. The specimens were further positioned in the reaction frame with the help of a chain pulley and placed properly. A manually operated hydraulic jack was used to apply the load gradually. A small rectangular plate was kept at the centre of the slab and a jack placed over it to reduce the gap between test slab and head of the loading jack (Figure 4 *b*). Both the specimens were placed one after another on the reaction frame; three dial gauges with least count of 0.01 mm were fixed at both acute corners

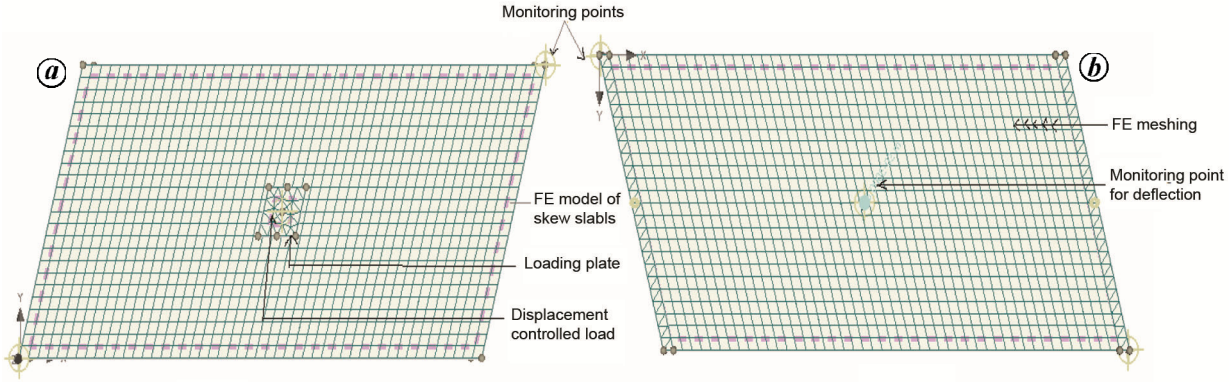

Figure 5. Finite element (FE) modelling of skew slab. (***a***) Top face with monitoring points at the corners. (***b***) Bottom face with monitoring points and supports.

and centre of the test slab with initial reading zero, to check uplift of the acute corners and deflection at the centre of the skew slab specimens. The initial load of 10 kN with the corresponding deflection of 2.2 mm was observed. The further increment of load was applied gradually by operating hydraulic jack, and deflection and uplift were recorded at different loads. Tensile zone of the slab was closely observed for development of cracks. The value at which the slab failed to carry any additional increase in the load was taken as the collapse load of the slab.

Numerical modelling of RC skew slabs

To validate the analytical and experimental studies, a numerical study using FE modelling was performed. Skew slabs were analysed as a 3D FE model using a software package (ATENA 3D). The user-defined cementitious material model in the software helps define real material behaviour exhibited by the concrete both in tension and compression. The skew slabs were modelled using a 3D solid brick element with eight nodes having six degrees of freedom at the individual nodes. The elemental constitutive model in the software was established by the smeared crack and damage approach, which is known as the crack band model based on Kufer's experiments. The geometry of the skew slab was established by defining individual solid regions known as macro-elements. Steel reinforcement was modelled as smeared with uniaxial properties oriented in the direction of the reinforcement based on a nonlinear model by Menegotto and Pinto[12].

In the present study, the macroelement-1 representing the RC skew slab and macro element-2 representing elastic layer were used to model the loading plate. The elastic layer exhibited a linear load–deflection response. Furthermore, the simply supported conditions were generated by restraining translation in the vertical direction at the two opposite edges of the bottom face of the skew slab. The software helps define real material behaviour exhibited by concrete in both tension and compression according to IS 456 guidelines[13]. The brick solid elements were selected for meshing the slab volume. The displacement-controlled loading was simulated by applying the loading in small displacement increments. This was applied to the macroelement-1. Forty load steps were defined to apply a total displacement of 50 mm at the centre of the slab. The load case consisting of vertical displacement was applied at the centrally placed node on the top face of the elastic layer (in the macroelement-2). Each load step was equivalent to a vertical displacement of 0.01 mm. The load applied in the form of vertical displacement to the macroelement-1 and vertical deflection shown by the slab at the midpoint of the bottom face of the slab (macroelement-1) were monitored by assigning a reaction-monitor and displacement-monitor on the nodes. Figure 5 *a* and *b* shows modelling of the skew slab and location of monitoring point respectively.

The software uses its automatic feature to determine the crack band size. The characteristic size used to estimate the strain in the material model was introduced as a fraction of the specimen size. The default value in ATENA was adopted as such in the present study. The Arc-Length option in ATENA solution parameters was used in the analysis, as this approach starts reducing automatically the applied loads to capture the true peak in the ultimate capacity. The standard Newton–Raphson method was employed for load steps only up to the level of the design load, and then the solution method switched to arc-length to capture the post-peak response of the collapsing slab. As the solution parameters in the nonlinear analysis have a significant effect on the accuracy of the simulated results, e.g. error in the equilibrium of forces, etc. therefore, several of trials were conducted by changing the default parameters in the software and examining its effect on the load–displacement response of the slab. The parameters giving consistent results were adopted in the study (Table 2). The default conditional break criterion in ATENA was adopted as such, without any modification, to stop the computation if an error

Table 2. Solution parameters adopted in the numerical analysis

Parameter (error tolerance)	Value	Parameter (error multiple)	Value	
			Break immediately	Break after step
Displacement error tolerance	0.010000	Displacement error multiple	10000.0	1000.0
Residual error tolerance	0.010000	Residual error multiple	10000.0	1000.0
Absolute residual error tolerance	0.010000	Absolute residual error multiple	10000.0	1000.0
Energy error tolerance	0.000100	Energy error multiple	1000000.0	10000.0

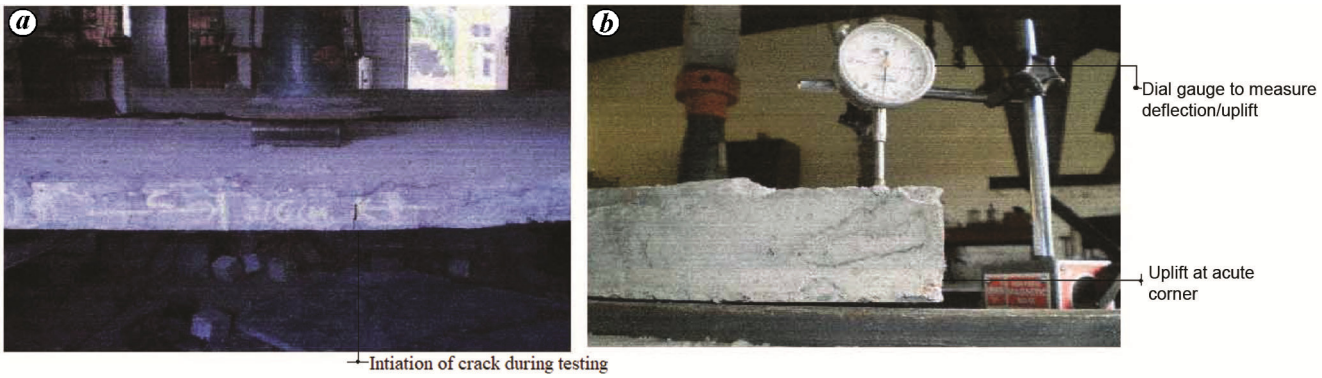

Figure 6. Skew slab testing in the laboratory. (***a***) Crack in the tensile face. (***b***) Uplift at acute corner.

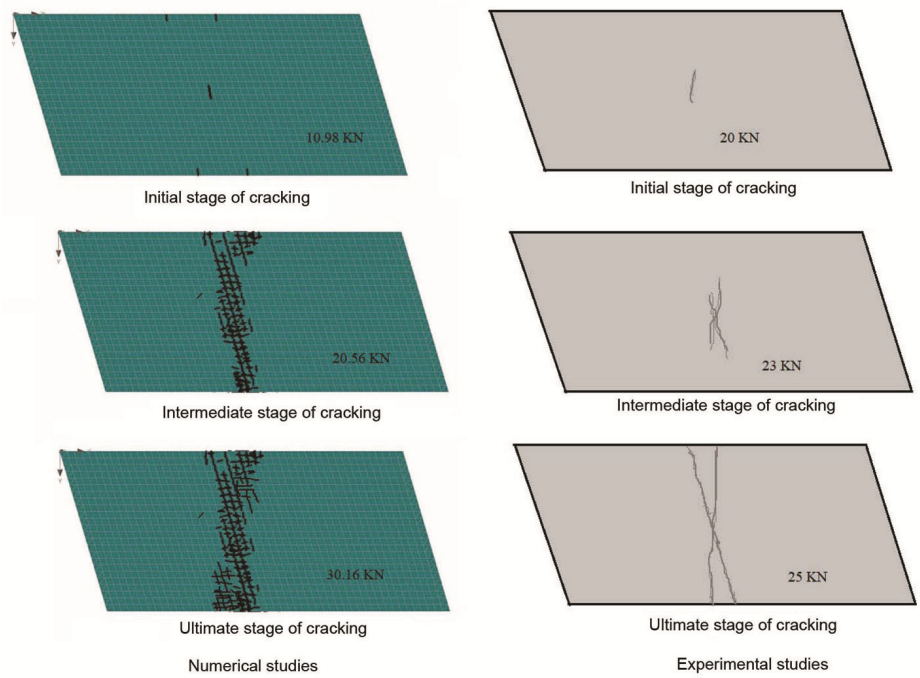

Figure 7. Collapse mechanism of the skew slab ($L < l$) during numerical and experimental studies at various stages.

exceeded the prescribed tolerance during iterations or at the end of an analysis step.

The size of the mesh was determined again by conducting a parametric study to observe how results from the model vary with the meshing element size. The numerically modelled slab was analysed at the different element sizes of tetrahedral solid elements. A compromised solution was found between the accuracy of the simulation and time taken in the analysis. An optimum mesh size of 25 mm was adopted in the analysis which gave almost

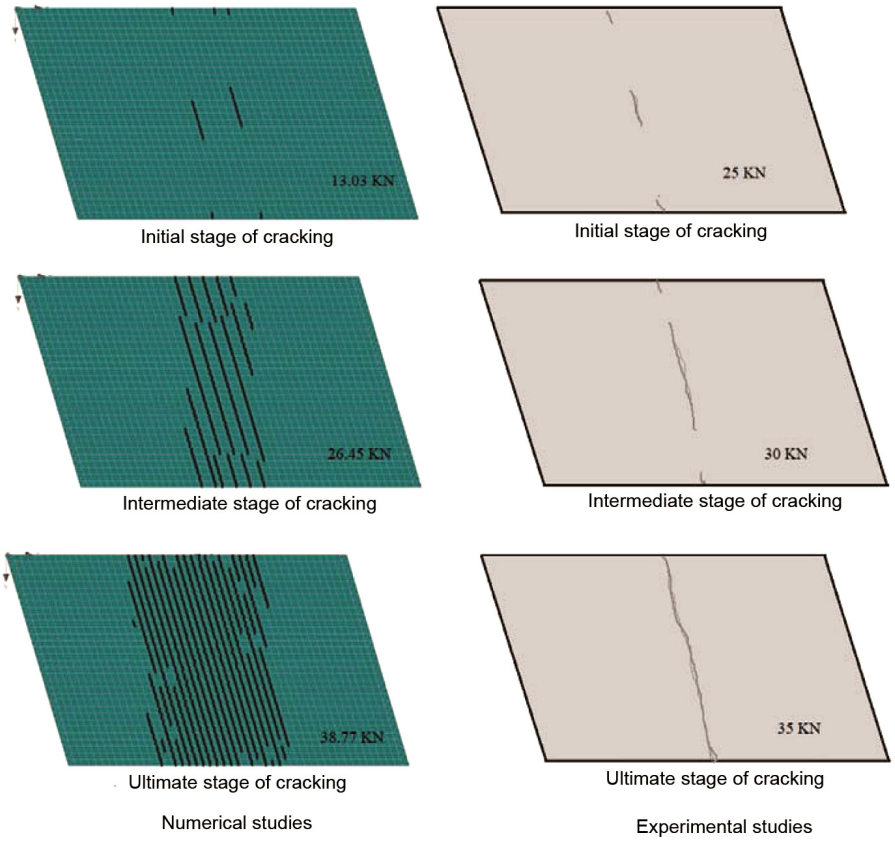

Figure 8. Collapse mechanism of the skew slab ($L > l$) during numerical and experimental studies at various stages.

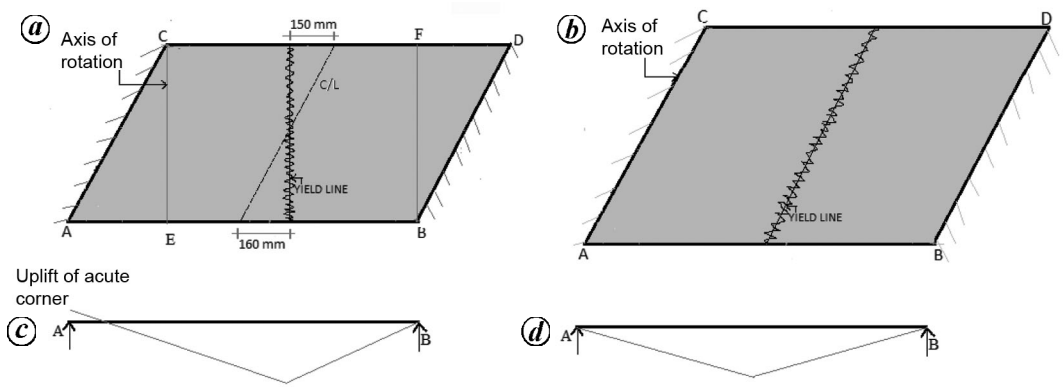

Figure 9. Collapse mechanism of the skew slab during experimental testing. (***a***, ***b***) Ultimate cracking stage: (***a***) ($L < l$) and (***b***) ($L > l$), (***c***, ***d***) Front elevation of deformable slab: (***c***) ($L < l$) and (***d***) ($L > l$).

identical crack initiation (Figure 6), collapse mechanism (Figures 7–9) and load-deflection (Figure 10) curves to experimental results for both the specimens.

Test results

Both the specimen were tested in the laboratory and analysed numerically. In the laboratory the skew slab specimens were tested under centrally placed concentrated load, whereas in software displacement-controlled load was applied at the centre on the top face of both specimens. Figures 7–10 show load/deflection behaviour and crack pattern for both the slabs.

Skew slab, $L < l$

Specimen 1 represents a skew slab with ratio of short diagonal to span less than unity ($L < l$). At collapse load

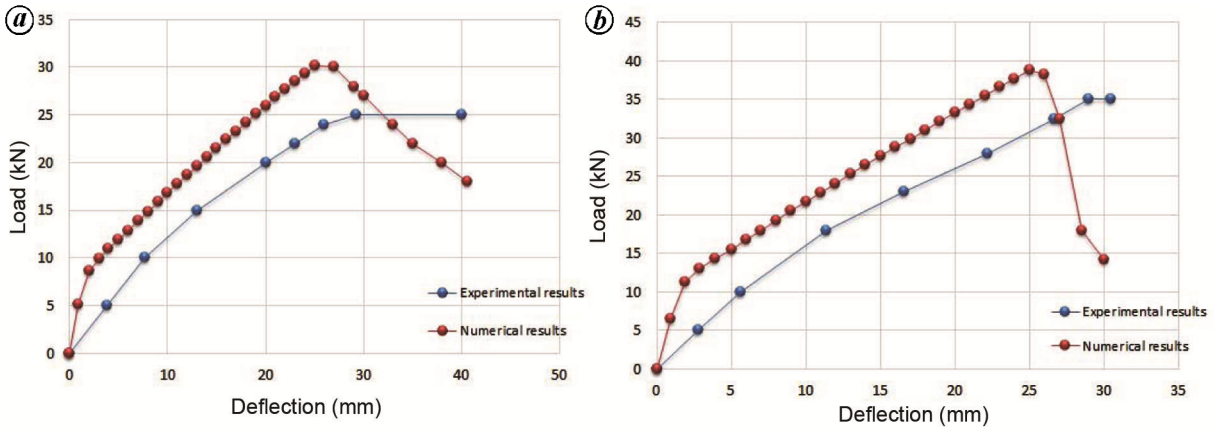

Figure 10. Load deflection response. (***a***) Skew slab specimen 1 ($L < l$). (***b***) Skew slab specimen 2 ($L > l$).

of 25 kN, the slab specimen showed lifting of acute corners by 1.65 mm with central deflection 40 mm, whereas in the numerical model maximum value of deflection of 40.59 mm was noticed under the maximum load of 30.16 kN, but maximum uplift at acute corners was noticed at 1.18 mm (Figure 6 *b*). In the case of analytical modelling, this load was found to be 25.04 kN. The load applied at the centre position of the small steel plate showed a strong resemblance with analytical and numerical analysis. In the initial phase of loading, the behaviour of the specimen was elastic. Invariably, the cracks began to initiate on the bottom face at the centre at load value of 20 kN. More fine cracks propagated gradually towards the end of the free edge on the tension face side as the loading progressed (Figure 6 *a*). Cracks developed at the bottom of the centre were not parallel to the supported edges, rather they were almost parallel to the axis of rotation at mid-span (Figure 9 *a* and *c*). The cracks shifted from the centre line towards the obtuse corners at the free edges. This shows that the reaction occurred at the obtuse corners only and the axis of rotation shifted from the supported edge and it passed through the obtuse corners (Figure 7) showed the comparison of collapse mechanism in numerical and experimental studies. Maximum crack size of 1.70 mm was noticed and it is was mm in case of numerical modelling whereas it was considered 0. 3 mm for analytical modelling. Figure 10 *a* shows the load–displacement curve. When the full crack pattern developed, the load started decreasing with an increase in deflection. The collapse load was 25 kN (experimentally) and 30.16 kN (numerically).

Skew slab, L > l

Length of the short diagonal of the slab was 2530 mm, which is greater than the span 2470 mm, representing the ratio of short diagonal to span greater than unity. When the point load was applied, no lifting of slab was observed at the supports or the corner, which shows that the reaction is well within the supports and the slab segments rotate about the supports, as predicted in the analytical modelling. Maximum load taken by slab was 35 kN experimentally and 38.77 kN numerically with corresponding deflection of 30.50 mm and 27.04 mm respectively, whereas it was 30 kN in case of analytical modelling. The crack developed at the bottom of the centre was parallel to the supported edges. The appearance of the first crack was initiated at the centre of the skew slab on the tension side. More cracks appeared at a load of 25 kN. These cracks gradually propagated towards the end of the free edges parallel to the supports on the tension face, as shown in Figure 8 and Figure 9 *b* and *d* and found similar as assumed for analytical modelling. Further full crack pattern replicated on paper, as shown in Figure 9 *b*. Maximum size of the crack is found to be 2.6 mm experimentally, and it was 3 mm in case of numerical modelling and 0.3 mm for analytical modelling. Figure 10 *b* shows load displacement curve Comparison of results for numerical and experimental studies given in Table 4 and found satisfactory. The average value of variation in experimental and numerical results with theoretical prediction was evaluated 0.92 and 0.79 respectively.

Determination of moment field/design chart for skew slabs using design equation

Indian Road Congress has provided details of simply supported bridges for span up to 14,000 mm in rural road manual. Generally, the width of single-lane and double lane slab bridges is kept 5150 mm and 7500 mm respectively, and maximum span up to 10,000 mm. Therefore, moment coefficients were generated using eq. (11), as shown in Table 3 and Figure 11. It shows only valid moment coefficients for various aspect ratio and skew angle. The value of moment coefficients has highlighted with bold values when the slab shows the lifting of acute

Table 3. Valid moment coefficients for skew angle 5°–70° and aspect ratio 0.3–3.

Skew angle/ aspect ratio	5	10	15	16.5	20	25	30	35	40	45	50	55	60	65	70
0.3	1.205	**1.219**	**1.243**	**1.252**	**1.277**	**1.324**	**1.386**	**1.465**	**1.567**	**1.698**	**1.868**	**2.093**	**2.401**	**2.841**	**3.510**
0.49	1.968	1.990	**2.030**	**2.045**	**2.086**	**2.163**	**2.264**	**2.394**	**2.560**	**2.773**	**3.051**	**3.419**	**3.922**	**4.640**	**5.733**
0.5	2.008	2.031	**2.071**	**2.086**	**2.129**	**2.207**	**2.310**	**2.442**	**2.612**	**2.830**	**3.113**	**3.488**	**4.002**	**4.735**	**5.850**
0.65	2.610	2.640	2.692	**2.712**	**2.767**	**2.870**	**3.003**	**3.175**	**3.395**	**3.678**	**4.047**	**4.535**	**5.202**	**6.155**	**7.606**
0.7	2.811	2.844	2.899	2.921	2.980	**3.090**	**3.234**	**3.419**	**3.656**	**3.961**	**4.358**	**4.884**	**5.603**	**6.629**	**8.191**
0.9	3.614	3.656	3.728	3.755	3.832	3.973	**4.158**	**4.396**	**4.701**	**5.093**	**5.603**	**6.279**	**7.203**	**8.522**	**10.531**
1	4.016	4.062	4.142	4.173	4.258	4.415	4.620	**4.885**	**5.224**	**5.659**	**6.226**	**6.977**	**8.004**	**9.469**	**11.701**
1.3	5.220	5.281	5.384	5.424	5.535	5.739	6.006	6.350	6.791	**7.357**	**8.093**	**9.070**	**10.405**	**12.310**	**15.211**
1.5	6.023	6.093	6.213	6.259	6.387	6.622	6.930	7.327	7.835	8.489	**9.338**	**10.465**	**12.006**	**14.204**	**17.551**
1.7	6.826	6.906	7.041	7.093	7.238	7.505	7.854	8.304	8.880	9.620	10.583	11.861	**13.606**	**16.098**	**19.892**
1.9	7.630	7.718	7.870	7.928	8.090	8.388	8.778	9.281	9.925	10.752	11.828	13.256	15.207	17.992	22.232
2	8.031	8.124	8.284	8.345	8.515	8.829	9.240	9.770	10.447	11.318	12.451	13.954	16.007	18.939	23.402
2.3	9.236	9.343	9.526	9.597	9.793	10.154	10.627	11.235	12.014	13.016	14.319	16.047	18.408	21.779	26.912
2.5	10.039	10.156	10.355	10.432	10.644	11.037	11.551	12.212	13.059	14.148	15.564	17.442	20.009	23.673	29.252
2.7	10.842	10.968	11.183	11.266	11.496	11.920	12.475	13.189	14.104	15.280	16.809	18.838	21.610	25.567	31.592
2.9	11.645	11.780	12.011	12.101	12.347	12.803	13.399	14.166	15.148	16.411	18.054	20.233	23.211	27.461	33.933
3	12.047	12.187	12.426	12.518	12.773	13.244	13.861	14.654	15.671	16.977	18.677	20.931	24.011	28.408	35.103

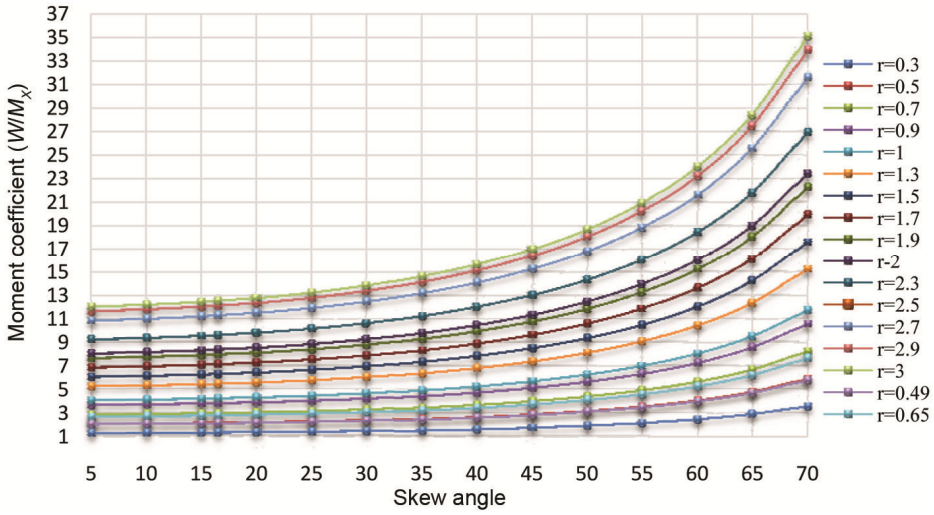

Figure 11. Design chart of moment coefficients for various skew angles and aspect ratios.

corners in Table 3. Collapse load in eq. (11) represents the total point load acting at the centre of the slab.

Skew slab, L < l

Span along the traffic, $l = 2470$ mm. Support length, $b = 1200$ mm; aspect ratio, $r = b/l = 0.49$, $\theta = 73.51°$; length of short diagonal, $L = 2420$ mm < span, $l = 2470$ mm. Collapse load of slab can be computed from eq. (7) after finding α_1

$$\alpha_1 = \frac{l^2\left(\begin{array}{c}4r\sin^2\theta\cos\theta + 4r^2\sin^2\theta\cos^4\theta + \\ (1-r\cos\theta)^2(1-\sin^2 2\theta)\end{array}\right)}{(l^2+b^2-2lb\cos\theta)},$$

$\alpha_1 = 1.08$. $M_X = 8.611$ kN-m. Therefore, $W = 19.00$ kN.

Actual collapse point load applied will be less than 19.00 kN, due to self-weight of the slab acting uniformly. The self-weight of the slab can be converted into equivalent point load acting at the centre by equating the moments produced by equivalent load and self-weight, i.e. by eqs (4) and (7). Self-weight of the slab, $w = 1.75$ kN/m^2. $Weq = 2.31$ kN.

Therefore, net point load that can be applied = 19.00–2.31 = 16.69 kN. Ultimate point load = 1.50 × 16.69 = 25.04 kN.

Skew slab, L > l

$r = b/l = 0.65$, $\theta = 73.51°$.

Table 4. Summary of results for skew slabs

	Analytical modelling	Numerical analysis		Experimental testing			
Skew slab specimen	Collapse load *Wa* (kN)	Collapse load *Wfe* (kN)	Uplift of acute corner	Collapse load *We* (kN)	Uplift of acute corner	*Wfe*/*Wa*	*We*/*Wa*
$L < l$	25.04	30.16	1.18	25.00	1.65	0.82	1.00
$L > l$	30	38.77	0	35.00	0	0.77	0.85

Short diagonal, L = 2530 mm > span, l = 2470 mm.

$$\frac{W}{M_X} = \frac{4r}{\sin\theta}.$$

Using Table 3, W = 23.35 kN.

Actual collapse point load applied will be less than 19.00 kN, due to self-weight of the slab acting uniformly. The self-weight of the slab can be converted into equivalent point load acting at the centre by equating the moments produced by equivalent load and self-weight, i.e. by eqs (10) and (11).

Net point load at collapse = 23.35 – 3.33 = 20.02 kN. M_X can be written as Weq = 3.33 kN. Ultimate point load = 1.50 × 20.02 = 30.03 kN.

Conclusion

(1) An analytical model has been proposed to design a skew slab with any skew angle and aspect ratio. Actual crack pattern and ultimate flexural capacity of the slab specimens, tested in the laboratory, was found to be in good agreement with theoretical predictions and simulated results.

(2) The behaviour of simply supported skew slabs under point load applied at the centre was found to depend on the ratio of short diagonal to its span. Skew slab with a ratio of short diagonal to span less than unity showed uplift of acute corners because the reactions acted at the obtuse corner only, and it was well within the supports when the ratio of short diagonal to span was greater than unity. Thus, the results do not recommend construction of skew slabs with short diagonal less than the span due to uplifting of acute corners. Also, the axis of rotation and yield line developed under concentrated load applied at the centre of skew slabs were not the same in the two types of skew slabs.

(3) Skew slabs with a ratio of short diagonal to its span less than unity showed lifting of acute corners; therefore, these are not recommended for construction. It is suggested that skew slabs with a ratio of short diagonal greater than unity should be constructed and by selecting suitable geometrical parameters, i.e. skew angle and aspect ratio. Otherwise, it is required to anchor the acute corners with supports, which will change its yield line pattern and the axis of rotation.

(4) Design aids have been suggested for analysis of simply supported skew slabs. These curves can be used for aspect ratios 0.3–3.0 and skew angles 5°–70°.

1. AASHTO, *LRFD Bridge Design Specifications*, American Association of State Highway and Transportation Officials, Washington DC, USA, 2007, 4th edn.
2. Menassa, C., Mabsout, M., Tarhini, K. and Frederick, G., Influence of skew angle on reinforced concrete slab bridges. *ASCE J. Bridge Eng.*, 2007, **12**(2), 205–214.
3. Ministry of Shipping and Transport (Road Wing), Government of India, In Standards Plans for Highway Bridges Vol. II. Concrete Slab Bridges, Indian Road Congress, New Delhi, 1983.
4. Bhatt, P., Abdel Hafiz, L. M. and Green, D. R., Direct design of reinforced concrete skew slabs. *Comput. Struct.*, 1988, **30**(3), 477–484.
5. Gupta, T. and Misra, A., Effect on support reactions of T-beam skew bridge decks. *ARPN J. Eng. Appl. Sci.*, 2007, **2**(1), 1–8.
6. Theoret, P., Massicotte, B. and Conciatori, D., Analysis and design of straight and skewed slab bridges. *ASCE J. Bridge Eng.*, 2012, **17**(2), 289–301.
7. Nouri, G. and Ahmadi, Z., Influence of skew angle on continuous composite girder bridge. *ASCE J. Bridge Eng.*, 2012, **17**(4), 617–623.
8. Jain, S. C. and Kennedy, J. B., Yield criterion of reinforced concrete slab. *J. Struct. Div. ASCE*, 1974, **100**(3), 631–644.
9. Muthu, K. U., Kamaranth, Ibrahim A and Mattarneh, H., Load deflection behaviour of partially restrained slab strips. *Eng. Struct.*, 2007, **29**, 663–674.
10. Gorkem, S. E. and Husem, M., Load capacity of high-strength reinforced concrete slabs by yield line theory. *Comput. Concr.*, 2013, **12**(6), 819–829.
11. BIS, IS 8112, Indian standard ordinary Portland cement 43 grade – specification, New Delhi, 2013.
12. Cervenka, V., Jendele, L. and Cervenka, J., *ATENA Theory Manual Part 1*, Cervenka Consulting, Prague, Czech Republic, 2011.
13. BIS, IS 456, Code of practice for the design of reinforced concrete structures, BIS, Bureau of Indian Standards, New Delhi, 2000.
14. IS 383, Specification for coarse and fine aggregates from natural sources for concrete, Bureau of Indian Standards, New Delhi, 1970.
15. IS IS10262, Recommended guidelines for concrete mix design, Bureau of Indian Standards, New Delhi, 2009.

Received 8 May 2019; revised accepted 24 February 2020

doi: 10.18520/cs/v118/i12/1911-1921